

The *SPTLC1* p.S331 mutation bridges sensory neuropathy and motor neuron disease and has implications for treatment

Chiara Fiorillo^{1,2}  | Giovanna Capodivento^{1,3} | Alessandro Geroldi¹ | Stefano Tozza⁴ | Isabella Moroni⁵ | Payam Mohassel⁶ | Matteo Cataldi^{1,7} | Chiara Campana⁷ | Simone Morando⁸ | Chiara Panicucci⁸ | Marina Pedemonte² | Noemi Brolatti² | Sabrina Siliquini⁹ | Monica Traverso² | Serena Baratto⁸ | Doriana Debellis¹⁰ | Stefania Magri¹¹ | Valeria Prada¹² | Emilia Bellone^{1,13} | Vincenzo Salpietro^{1,2} | Sandra Donkervoort⁶ | Kenneth Gable¹⁴ | Sita D. Gupta¹⁴ | Teresa M. Dunn¹⁴ | Carsten G. Bönnemann⁶ | Franco Taroni¹¹ | Claudio Bruno⁸ | Angelo Schenone^{1,3} | Paola Mandich^{1,13} | Lucilla Nobbio^{1,3}  | Maria Nolano^{4,15}

¹Department of Neuroscience, Rehabilitation, Ophthalmology, Genetics and Maternal and Child Health (DINO GMI), University of Genoa, Genoa, Italy

²Unit of Paediatric Neurology and Neuromuscular Disorders, IRCCS Institute "G. Gaslini", Genoa, Italy

³UO Clinica Neurologica, IRCCS Ospedale Policlinico San Martino, Genoa, Italy

⁴Department of Neuroscience, Reproductive and Odontostomatological Science, University of Naples "Federico II", Naples, Italy

⁵Child Neurology Unit, Department of Pediatric Neuroscience, Fondazione IRCCS Istituto Neurologico Carlo Besta, Milan, Italy

⁶Neuromuscular and Neurogenetic Disorders of Childhood Section, National Institute of Neurological Disorders and Stroke, National Institutes of Health, Bethesda, Maryland, USA

⁷Paediatric Neuropsychiatric Unit, IRCCS Institute "G. Gaslini", Genoa, Italy

⁸Center of Translational and Experimental Myology, IRCCS Institute "G. Gaslini", Genoa, Italy

⁹Paediatric Neuropsychiatric Unit, Ospedali Riuniti, Ancona, Italy

¹⁰Electron Microscopy Facility, Istituto Italiano di Tecnologia, Genoa, Italy

¹¹Unit of Medical Genetics and Neurogenetics, Fondazione IRCCS Istituto Neurologico Carlo Besta, Milan, Italy

¹²Department of Neurology, University of Iowa, Iowa City, Iowa, USA

¹³Clinical Genetics Unit, Ospedale Policlinico IRCCS San Martino, Genoa, Italy

¹⁴Department of Biochemistry and Molecular Biology, Uniformed Services University of Health Sciences, Bethesda, Maryland, USA

¹⁵Neurology Department, Skin Biopsy Laboratory, Istituti Clinici Scientifici Maugeri IRCCS, Telesse Terme, Italy

Correspondence

Chiara Fiorillo, Department of Neuroscience, Rehabilitation, Ophthalmology, Genetics and Maternal and Child Health (DINO GMI), University of Genoa, Genoa, Italy.
Email: chiara.fiorillo@edu.unige.it

Abstract

Aims: *SPTLC1*-related disorder is a late onset sensory-autonomic neuropathy associated with perturbed sphingolipid homeostasis which can be improved by supplementation with the serine palmitoyl-CoA transferase (SPT) substrate, L-serine. Recently, a juvenile form of motor neuron disease has been linked to *SPTLC1* variants. Variants affecting the p.S331

Chiara Fiorillo and Giovanna Capodivento equally contributed as first authors.

Lucilla Nobbio and Maria Nolano equally contributed as last authors.

This is an open access article under the terms of the [Creative Commons Attribution-NonCommercial-NoDerivs](https://creativecommons.org/licenses/by-nc-nd/4.0/) License, which permits use and distribution in any medium, provided the original work is properly cited, the use is non-commercial and no modifications or adaptations are made.

© 2022 The Authors. *Neuropathology and Applied Neurobiology* published by John Wiley & Sons Ltd on behalf of British Neuropathological Society.

Funding information

Care4NeuroRare, Grant/Award Number: CP 20/2018; French Muscular Dystrophy Association, Grant/Award Number: 22431; Italian Ministry of Health Ricerca corrente 2018-2021

residue of *SPTLC1* cause a distinct phenotype, whose pathogenic basis has not been established. This study aims to define the neuropathological and biochemical consequences of the *SPTLC1* p.S331 variant, and test response to L-serine in this specific genotype.

Methods: We report clinical and neurophysiological characterisation of two unrelated children carrying distinct p.S331 *SPTLC1* variants. The neuropathology was investigated by analysis of sural nerve and skin innervation. To clarify the biochemical consequences of the p.S331 variant, we performed sphingolipidomic profiling of serum and skin fibroblasts. We also tested the effect of L-serine supplementation in skin fibroblasts of patients with p.S331 mutations.

Results: In both patients, we recognised an early onset phenotype with prevalent progressive motor neuron disease. Neuropathology showed severe damage to the sensory and autonomic systems. Sphingolipidomic analysis showed the coexistence of neurotoxic deoxy-sphingolipids with an excess of canonical products of the SPT enzyme. L-serine supplementation in patient fibroblasts reduced production of toxic 1-deoxysphingolipids but further increased the overproduction of sphingolipids.

Conclusions: Our findings suggest that p.S331 *SPTLC1* variants lead to an overlap phenotype combining features of sensory and motor neuropathies, thus proposing a continuum in the spectrum of *SPTLC1*-related disorders. L-serine supplementation in these patients may be detrimental.

KEYWORDS

HSAN, L-serine, motor neuron, S331, sphingolipids, SPTLC1

INTRODUCTION

SPTLC1 gene encodes the subunit 1 of serine palmitoyltransferase (SPT), a multi-subunit enzyme that catalyses the condensation of L-serine with fatty acyl-CoA (commonly, palmitoyl-CoA) to form long-chain bases. This is the first and rate-limiting step in the de novo biosynthesis of sphingolipids.¹ SPT activity requires close homeostatic regulation to ensure adequate sphingolipid synthesis and to prevent cell toxicity.² Perturbed sphingolipid metabolism underlies many neurological disorders, including CMT1A, Niemann–Pick disease and Gaucher disease.³

Pathogenic variants in *SPTLC1* have been classically associated with Hereditary Sensory and Autonomic Neuropathy type I (HSAN1), one of the most common inherited disorders of the peripheral sensory neurons. HSAN1 is a debilitating neuropathy characterised by marked sensory involvement and variable motor and autonomic impairment usually manifesting between the second and third decade of life.^{4,5}

HSAN1-associated *SPTLC1* variants (typically involving C133, V144 or A352 residues) reduce the canonical enzymatic activity, with a shift in the substrate specificity from serine toward L-alanine and glycine.⁶ This shift results in the formation of atypical 1-deoxysphingolipids (1-deoxySLs) that cannot be converted into more complex SLs and are not efficiently degraded. These toxic SLs accumulate in the serum of HSAN1 patients, and in HSAN cellular and animal models with pronounced neurotoxic effects on neurite formation of sensory neurons.^{7,8}

Key Points

- Novel sphingolipidomic and neuropathological findings in p.S331 mutation carriers suggest a continuum in the spectrum of *SPTLC1*-related disorders.
- L-serine supplementation in skin fibroblasts from p.S331 mutated patients displays a detrimental effect on sphingolipid homeostasis.
- Mutations affecting the S331 residue of *SPTLC1* cause a distinct phenotype, which has implications for treatment.

A recent clinical trial in adults with HSAN1 showed that oral L-serine supplementation improves the biochemical abnormalities by reducing circulating 1-deoxySL levels and results in an increase in epidermal innervation. Thus, oral L-serine supplementation can be considered an effective therapy to slow HSAN1 disease progression.⁹

Recently, *SPTLC1* has also been associated with childhood onset amyotrophic lateral sclerosis (ALS) with a different metabolic pathogenicity to HSAN1.¹⁰ These distinct ALS causing variants, all localised in exon 2 of *SPTLC1*, result in an up-regulation of SPT activity and increased levels of canonical SPT products, without production of 1-deoxySLs.

Lastly, several reports suggest the existence of a third distinct phenotype related to pathogenic variants that alter residue p.S331 of *SPTLC1*, the so-called ‘S331 syndrome’. Three patients carrying the p.S331F variant and two patients carrying the p.S331Y variant have

TABLE 1 Literature summary of clinical, histopathological and biochemical features of patients carrying SPTLC1 Ser331 variants

	P1	Auer-Grumbach et al., 2013	Rossi et al., 2020	P2	Rotthier et al., 2010	Rotthier et al., 2009	Suh et al., 2014	Jonson et al., 2021
Mutation	S331Y	S331Y	S331Y	S331F	S331F	S331F	S331F	S331F
Origin	Italy	-	Sri Lanka	Italy	German	French (gypsy)	Korean	African American
Sex	Female	Female	Male	Female	-	-	Male	Female
Age at onset	5 years old	4 years old	4 years old	Neonatal	Early childhood	Congenital	5 years old	4 years old
Age at last evaluation	14 years old	14 years old	14 years old	6 years old	-	7 years old	28 years old	11 years old
Sensory symptoms	Yes	No	No	Yes	Yes	Yes	Yes	Yes
Foot ulcerations/ amputation	No	Yes	No	No	Yes	Yes	Yes	No
Autonomic system symptoms	No	No	Gastrointestinal involvement	Delayed gastric emptying. Lack of sweating and keratoconjunctivitis sicca	-	Gastro-oesophageal reflux	No	Yes
Juvenile cataract	No	Yes	Yes	Yes	Yes	No	Yes	No
Diffuse muscular atrophy	Yes	Yes	Yes	Yes	Yes	Yes	Yes	Yes
Wheel chair dependence	Yes (12 years old)	Yes (14 years old)	Yes (8 years old)	No	-	-	No	No
Pes cavus/ft deformities	Yes	Yes	Yes	Yes	-	No	-	-
Scoliosis	Yes	Yes	Yes	No	-	-	Yes	-
Upper motor neuron signs	Yes	Yes	Yes	Yes	-	No	No	Yes
Vocal cord paralysis/ hoarseness	Yes	-	-	No	-	Yes	Yes	-
Tongue fasciculations	Yes	Yes	Yes	No	-	-	-	Yes
Respiratory involvement	Yes	Yes	Yes	No	-	Yes	Yes	No
Growth retardation	No	Yes	Yes	Yes	-	Yes	-	Yes
Mental retardation	No	No	No	No	-	Yes	-	No

(Continues)

TABLE 1 (Continued)

	P1	Auer-Grumbach et al., 2013	Rossi et al., 2020	P2	Rotthier et al., 2010	Rotthier et al., 2009	Suh et al., 2014	Jonson et al., 2021
Plasma sphingolipids dosage	Increased 1-deoxySL AND canonical SPT products	Increased 1-deoxySL	-	Increased 1-deoxySL AND canonical SPT products	Increased 1-deoxySL	Increased 1-deoxySL	-	-
Nerve conduction study	SM Severe demyelinating UL and LL Absent sensory responses LL	SM Mixed demyelinating and axonal neuropathy	SM Mixed demyelinating and axonal neuropathy	Mixed axonal and demyelinating length dependent neuropathy	SM axonal	SM Absent responses UL/LL	SM Mixed demyelinating and axonal UL Absent responses LL	SM axonal neuropathy
Muscle MRI	Severe atrophy with fatty replacement of leg muscles and most of thigh muscles	-	-	Atrophy and fatty replacement of distal leg muscles	-	-	-	-
Muscle biopsy	-	-	-	Predominance of type 1 fibres. Denervation	-	-	-	-
Nerve biopsy	Complete absence of myelinated fibres. Signs of axonal deterioration	-	-	-	Marked wasting of myelinated fibres, unmyelinated fibres were present	-	-	-
Skin biopsy	Complete loss of epidermal nerve fibres. Autonomic denervation	-	-	Complete loss of epidermal nerve fibres. Autonomic denervation more severe than S331Y	-	-	-	-
Fibroblast response to L-serine	Reduced 1-deoxySA and 1-deoxyCer, no effect on sphinganine and total ceramide	-	-	Increased the levels of sphinganine and total ceramide. No effect on deoxy SL	-	-	-	-

Note: “-” not performed or not mentioned.

Abbreviations: SM, sensory motor; UL, upper limb; LL, lower limb.

been described, manifesting with a severe phenotype characterised by early onset neuropathy, prominent muscle atrophy, growth retardation, and oculo-skeletal abnormalities.^{4,11–13}

Biochemical findings from *in vitro* studies on p.S331 variants appear distinct from typical HSAN1 variants and highlight not only production of 1-deoxySLs but also an increase in canonical SPT activity with increased formation of C18- and C20-sphingoid base SLs.¹⁴ The underlying pathomechanism for the different clinical and biochemical phenotype of the p.S331 variants has not been fully elucidated, and thus it remains unclear if this subset of patients with *SPTLC1* mutations would benefit from serine supplementation.

Here, we performed an in-depth study of clinical, neurophysiology, histopathological and biochemical features of 2 Italian unrelated children aged 14 and 6, carrying p.S331Y and p.S331F variant of *SPTLC1*, respectively. We also tested patient-derived skin fibroblasts for possible effect of L-serine supplementation on SLs production.

MATERIALS AND METHODS

Subjects

Patients were evaluated by neuromuscular specialists at third level paediatric hospitals. Charcot-Marie-Tooth disease Pediatric Scale (CMTPedS) was administered by expert physiotherapists. Nerve conduction studies (NCS), electromyography (EMG) and sympathetic skin response were performed by expert neurophysiologists according to standard procedures. Muscle MRI protocol included axial T1 section of lower limb with 1.5 T machinery. Each patient underwent two different skin biopsies for histopathological examination and fibroblast culture, respectively. A skin biopsy was also obtained during an orthopaedic intervention by a paediatric healthy subject and used as control. Muscle biopsy was performed in Patient 2 from the left quadriceps and processed with standard histopathological stains. Sural nerve biopsy was performed in Patient 1 in conjunction with surgery for correction of foot deformities and was processed for light and electron microscopy. Moreover, an archived sural nerve biopsy from an unaffected paediatric subject who underwent nerve biopsy for suspected peripheral neuropathy was used as control. An overview of our patients' characteristics and a comparison with the literature is displayed in Table 1. Written informed consent for the above-mentioned research studies and for image use was obtained from patients' parents according to WMA Helsinki Declaration 2013.

Genetics

Genetic studies were performed with a Next Generation Sequencing (NGS) custom panel, using Illumina (Patient 1 with p.S331Y variant) and Ion Torrent technology (Patient 2 with p.S331F variant). In both cases, a panel spanning most of the hereditary neuropathies genes was designed respectively through Nextera Rapid Capture Custom kit (Illumina) and Custom Ion AmpliSeq sNGS Panels (ThermoFisher).

Libraries were run on a MiSeq Illumina sequencer (Illumina) and Ion GeneStudio S5 System (ThermoFisher). Bioinformatic analyses were carried out through MiSeq Reporter and VariantStudio software (Illumina), and Ion Reporter (ThermoFisher) and Wannovar.¹⁵

Neuropathology

Skin biopsy

A single biopsy from hairy skin was obtained using a 3 mm punch from a distal site of both the patients and control subject, fixed in Zamboni solution and transferred in a cryoprotectant. Free-floating 50 μ m-thick sections were processed for indirect immunofluorescence using a panel of primary antibodies against neural structures: the pan-neuronal marker protein gene product 9.5 (PGP), myelin basic protein (MBP; to assess myelinated fibres), vasoactive-intestinal-peptide (VIP; to assess cholinergic fibres), and dopamine-beta-hydroxylase (D β H; to assess noradrenergic fibres).¹⁶ Vascular bed and basal membranes were marked with antibody against collagen IV (COLIV), and endothelia and epidermis with *Ulex europaeus* agglutinin 1. Species-specific secondary antibodies coupled with cyanine 2 and cyanine 3 fluorophores were used. Digital images were acquired using a non-laser confocal microscope (Apotome; Zeiss).

Sural nerve biopsy

Sural nerve biopsy of Patient 1 was taken under sterile conditions and divided into two segments, one of which was paraformaldehyde-fixed, embedded in paraffin and processed for immunohistochemistry. In particular, five-micrometre-thick longitudinal and transverse sections were stained with Mallory trichrome following manufacturer's instructions (Bio-Optica 04-020802). Images were taken with an Olympus PROVIS AX60 microscope, connected to an Olympus DP70 digital camera.

The other segment was fixed in 2.5% glutaraldehyde in cacodylate buffer, pH 7.4, for 24 h and embedded in Epon for light and electron microscopy analyses.¹⁷ In particular, for light microscopy semi-thin sections were cut, stained with toluidine blue and analysed with an Olympus PROVIS AX60 microscope, connected to an Olympus DP70 digital camera. For transmission electron microscopy (TEM) analysis, 70 nm ultra-thin sections were cut and stained with 1% uranyl acetate and lead citrate solution. Images were collected with a Jeol JEM 1011 (Jeol, Japan) electron microscope, operating with a maximum acceleration voltage of 100 kV and recorded with a 2 Mp charge-coupled device camera (Gatan Orius SC100).

Sphingolipidomic analysis of serum and fibroblasts

Sample preparation and analysis were performed as previously described.¹⁸ In brief, serum (20 μ l) or cell pellets (~0.1–0.2 mg of protein) were mixed with internal SLs standards (Avanti Polar Lipids,

LM6002) and lipids were extracted and prepared for HPLC. The samples were analysed using an Agilent 1200 Series HPLC coupled to an ABSciex QTRAP 4000 MS. The mass spectrometer was set to detect compounds in multiple reaction monitoring (MRM) mode, and compounds were quantified based on the ratio of the peak to the known concentration of the representative internal standard using the ABSciex Analyst program.¹⁸

For assessment of de novo SL synthesis experiments, deuterium-labelled amino acids (3,3-D₂ L-serine, DLM-161 or D₄ L-alanine, Cambridge Isotope Laboratories) were added 24 h before harvesting the cells. Cells were trypsinised and reconstituted in PBS and divided into glass tubes for lipid extraction and Eppendorf tubes for protein quantification using the BCA assay (Thermo Fisher). Results for each sample were normalised to protein concentration (or volume for serum). D₂ labelled sphingomyelin (SM) measurements were corrected for the naturally prevalent +2 sphingomyelin species (~8.5%).

For total long chain base quantification, 1 ml 1 M HCl : methanol (Supelco) containing 32.5 pmol C17:1 LCB (as internal standard) was added to 20 µl serum in glass tubes and the samples were boiled in a water bath for 60 min. After addition of 1 ml 1% NaCl, the solution was extracted with 2 ml hexane : diethyl ether (1:1) and spun to separate the phases. The upper organic phase was removed by aspiration and discarded; 0.25 ml 10 M NaOH was added to the lower aqueous phase and after mixing, and the LCBs were extracted into 2 ml of hexane by vortexing and centrifugation to separate the phases. From the upper organic phase, 1.5 ml was collected, dried under N₂ and redissolved in 0.25 ml LC/MS solvent. Typically, 5 µl were injected, normalised to the internal standard and quantified using a separate injection of known standards.

RESULTS

Clinical information

Patient 1

A 12-year-old Italian girl was admitted for evaluation of sensory-motor neuropathy. She was the first child of healthy, unrelated parents. Motor development was normal, as was her weight and height. From the age of 4 years, difficulties in running and climbing stairs and unspecific discomfort during clipping her fingernails and brushing hair were noted with a neurological examination reporting tip-toe walking and brisk reflexes, and with normal brain and spine MRI. Motor defects became more evident with overt distal muscle weakness and atrophy, bilateral steppage, hand tremor and *pes cavus*. NCS at age 8 years documented a mixed demyelinating and axonal neuropathy more severe in the lower limbs. Genetic investigation excluded *PMP22* duplication, and a subsequent NGS panel for known forms of hereditary neuropathies identified a de novo p.S331Y variant in *SPTLC1* (Figure 1A).

Progressive muscle weakness with notable hand dysfunction and tongue fasciculation started at age 10 with a loss of ambulation at age 12. Burning pain in the lower limbs was also noted at same age,

successfully treated with gabapentin. Additionally, dorso-lumbar scoliosis and progressive foot *equino-varus* deformation emerged that was surgically treated. Nocturnal ventilation was started at age 12 for a restrictive respiratory dysfunction.

There was no clinical concern for cognitive, cardiac or gastrointestinal involvement. Ocular examination and electrocardiogram were normal.

Her most recent neurological examination at age 14 years showed moderate weakness in the proximal muscles (Medical Research Council, MRC 3/5) and severe weakness in her distal muscles (MRC 1-2/5), with atrophy, *pes cavus* and contractures of the hands and fingers; atrophy and fasciculation of the tongue were also present (Figure 2A–C). The patient could not raise her arms above her shoulders, and she was not able to walk nor maintain an upright posture without a harness or assistance. Pan modal hypoaesthesia of the hands and feet was also present. Tendon reflexes were absent. The CMTpedS score was 37/44.

No motor or sensory potentials were recordable with NCS, and the sympathetic skin response amplitude was very low. Severe and diffuse fatty replacement in the leg and posterior compartment of the thigh was evident on muscle MRI (Figure 2D).

Patient 2

The second proband was a 4-year-old Italian girl who came to our attention for a possible myopathy. She was the only child of unrelated, healthy parents. Pregnancy and delivery were uneventful. Club feet and global hypotonia were present in the first months and ambulation was achieved at 20 months (Figure 2E). In addition, since age of 5 months, a flattened growth rate was reported as due to frequent vomiting and delayed gastric emptying, requiring nasogastric tube feeding for several months. These symptoms resolved around 2 years of age, albeit that growth parameters remained below the third percentile. At that time, eye evaluation revealed multiple corneal abrasions, dystrophic corneal epithelium and early cataract. A muscle biopsy of the left quadriceps was performed at age 3 years, which showed fibre-type grouping and the presence of angular atrophic fibres suggesting acute and chronic neurogenic change (Figure 2F).

At first visit to our hospital, the neurological examination documented normal cognitive function and cranial nerves, diffuse muscle hypotonia and joint laxity, absent reflexes but brisk patellar reflex. Ambulation was very impaired due to ankle contractures and club feet with hammer toes. She needed support to climb stairs and showed a positive Gowers' sign. Pan-modal hypoaesthesia was evident in her distal lower limbs.

Increased duration of motor unit action potentials in the tibialis anterior muscle was observed on needle electromyography (15.9 ms; + 59% SD), in keeping with a severe rearrangement of MUAPs due to axonal loss. A nerve conduction study showed reduced motor and sensory nerve conduction velocities, suggestive of a length-dependent demyelinating neuropathy.

Genetic investigations with a dedicated NGS panel for hereditary neuropathies revealed a de novo p.S331F variant in *SPTLC1* (Figure 1B).

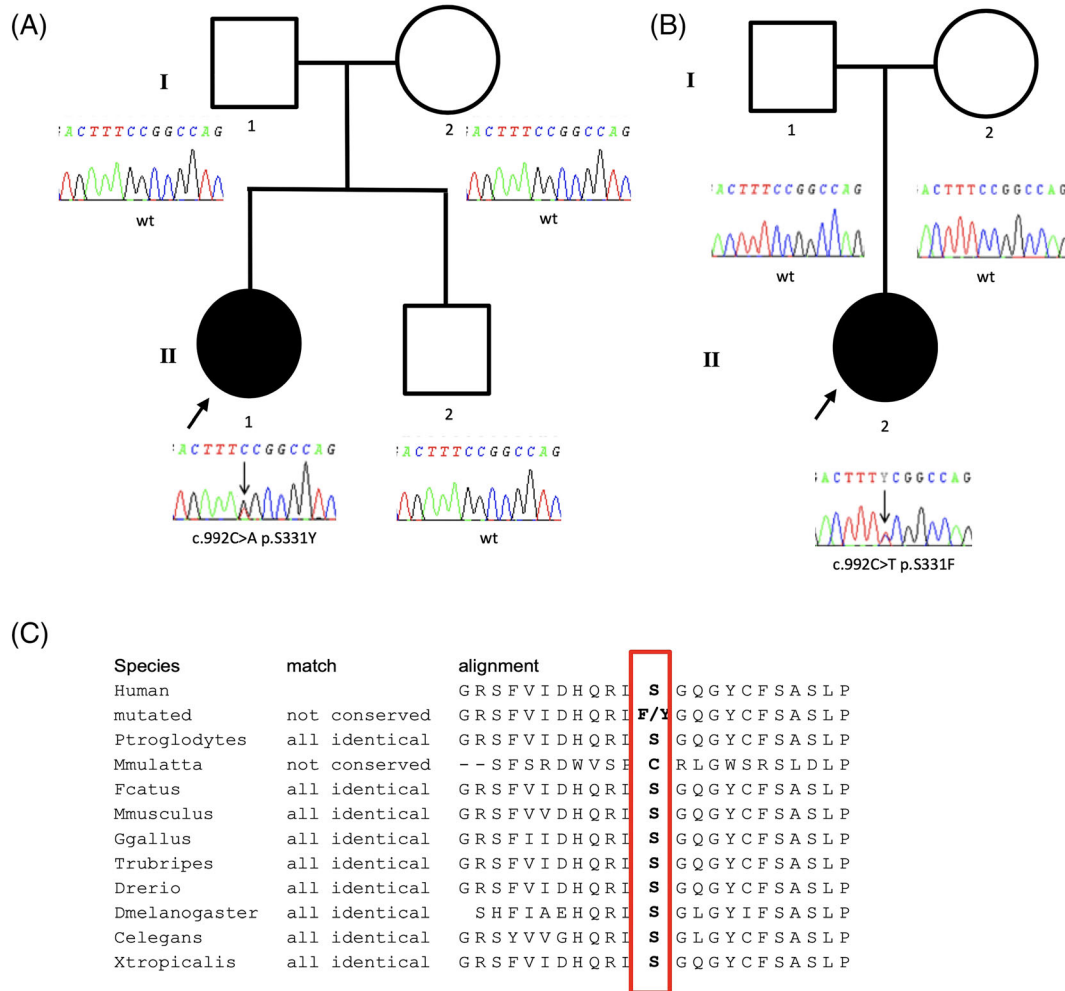


FIGURE 1 Pedigree and sequencing chromatogram of the *SPTLC1* gene mutation. Family 1 (panel A) and family 2 (panel B). The proband is indicated by an arrow. Vertical arrows indicate the mutation site. Conservation analysis of the amino acid sequences between different species (panel C)

Last examination at age 6 was unchanged except for reduced patellar tendon reflexes, mild weakness of hand fingers extension (MRC 4/5) and more severe thermal sensation impairment in the hands and feet. Moreover, slowly healing pressure sores on the feet and total absence of sweating (even at very high ambient temperatures) were reported. The CMTPedS score was 18/44.

A further eye evaluation documented diffuse punctate keratopathy (Oxford score 4), corneal ulceration and severe lacrimal hyposalivation, compatible with the diagnosis of keratoconjunctivitis sicca.

Muscle MRI documented early fatty replacement of the tibialis anterior muscle in its distal portion and the vasti muscles at the knee level.

Neuropathological investigations

Skin innervation

Cutaneous innervation appeared severely affected in both patients. In particular, we observed a complete lack of epidermal nerve

fibres (ENF - empty arrowheads in A1), with the occurrence of intra-papillary nerve fibres mostly located around the capillary loops. Few fibres were observed around hair follicles with a very simplified pattern (Figure 3B1, C1) compared with control (Figure 3A1).

Dermal adnexal innervation appeared poor (2/4 using a semi-quantitative approach) on PGP9.5-stained sections and severely affected, with faint staining, on sections stained with selective autonomic noradrenergic (DbH-ir) and cholinergic (VIP-ir) markers (not shown). Autonomic denervation was more severe in Patient 2 (p.S331F) (Figure 3C2, C3) compared with that in Patient 1 (p.S331Y) (Figure 3B2, B3). For both patients, no myelinated fibres (MBP-ir) were found in the dermal plexus or around the hair follicles (data not shown).

Overall, somatic (myelinated and unmyelinated) nerves fibres appeared more severely affected than autonomic nerve fibres, whose involvement was however more evident when observing selective cholinergic and noradrenergic immunoreactivity and particularly severe in Patient 2.

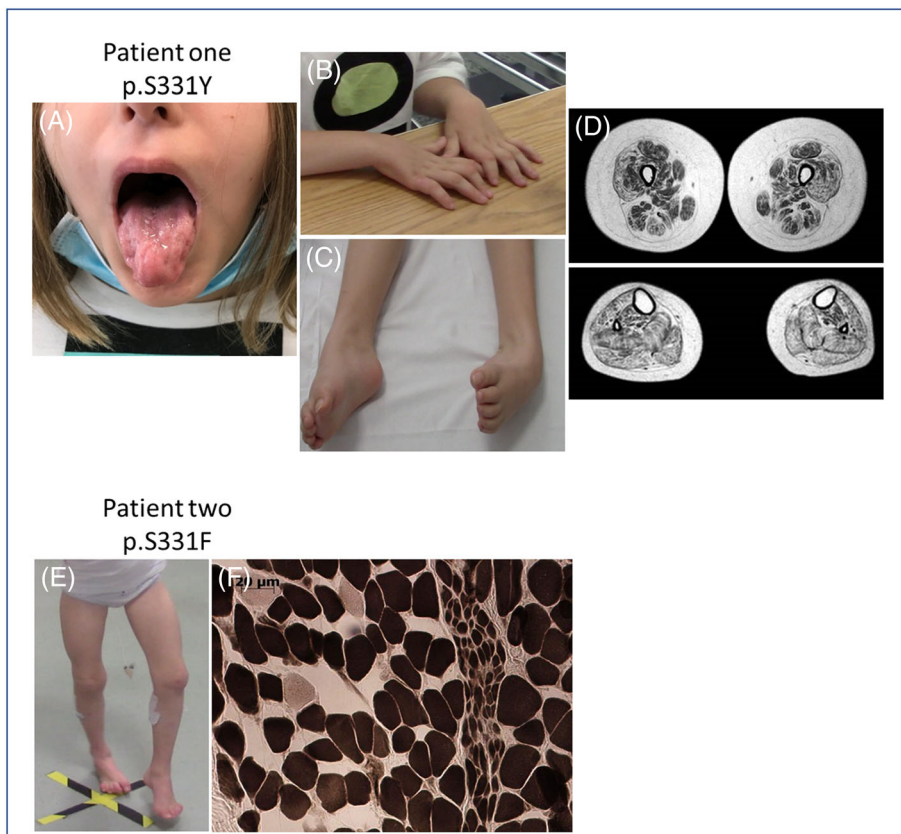


FIGURE 2 Summary of the clinical features from patients with p.S331 mutations in the *SPTLC1* gene. (A–D) Patient 1 with *SPTLC1* p.S331Y variant. (A) Tongue atrophy and fasciculation; (B, C) hands and foot deformities; (D) T1 axial MRI images of lower limbs muscles showing diffuse fatty replacement (T1 hyperintensity) of all leg muscles (lower panel) and most of the muscles in the thigh (upper panel), with partial preservation of quadriceps and adductors. (E, F) Patient two with *SPTLC1* p.S331F variant. (E) Low stature and diffuse muscle hypotrophy with *pes cavus*; ambulation is still possible. (F) Muscle biopsy from the quadriceps (*vastus lateralis*) muscle. ATP staining at pH 4.3 shows predominance of type 1 dark fibres. A denervated fascicle is also spotted with atrophic angulated fibres. Bar = 20 μ m

Sural nerve

Sural nerve biopsy from Patient 1 (p.S331Y) showed a severe picture compared with the control displaying a complete depletion of myelinated fibres, consistent with typical HSAN1 (Figure 4A,C). Nerve staining for myelin and connective tissue confirmed the almost complete loss of myelin membranes and a remarkable increase of collagen fibrils especially inside the endoneurium (Figure 4B,D).

Electron microscopy better detailed the severe neuropathological phenotype and confirmed the almost complete absence of myelinated fibres (Figure 4E,F). Only one degenerating myelinated fibre was found with clear signs of axonal damage as outlined by detachment from myelin membrane; we did not find any increase of inflammatory cells or onion bulbs. Unmyelinated fibres appeared mainly preserved (Figure 4G). We also found typical collagen-pocket structures and an increased number of mitochondria (Figure 4G).

Biochemical analyses

Serum sphingolipidomic profile

Sphingolipidomic assessment of serum samples from both patients was compared with healthy controls. Similar to what is reported in the literature for classic HSAN1 patients, both patients showed significant

elevation of 1-deoxy and 1-deoxymethyl ceramides (Figure 5A). To compare total levels of different SLs with the same long chain base backbone, we quantified long chain base levels in serum samples after acid hydrolysis and compared the findings to healthy controls and two classic HSAN1 patients (with the *SPTLC1* p.C133 variant). This analysis also showed that 1-deoxy and 1-deoxymethyl SLs were significantly elevated in both p.S331 variant samples. The classic HSAN1 samples showed mixed results. Whereas 1-deoxymethyl SLs were elevated in both (although to a lesser degree compared with p.S331 samples), 1-deoxy SLs were elevated in only one of the classic HSAN1 samples compared with control (Figure 5B).

In addition, the acid hydrolysed samples were analysed for canonical SL species. The canonical 18-carbon sphingoid base containing SLs did not differ between p.S331 and control samples. However, in classic HSAN1 samples, they were reduced, consistent with decreased activity of *SPTLC1* p.C133W variant-containing SPT complex 5. In contrast, the 20-carbon sphingoid base containing SLs were elevated in S331 patient serum samples (Figure 5C).

De novo SLs synthesis and response to L-serine supplementation in patients' fibroblasts

We also assessed the de novo rates of SLs and 1-deoxySLs synthesis, and response to exogenously-added serine in patient-

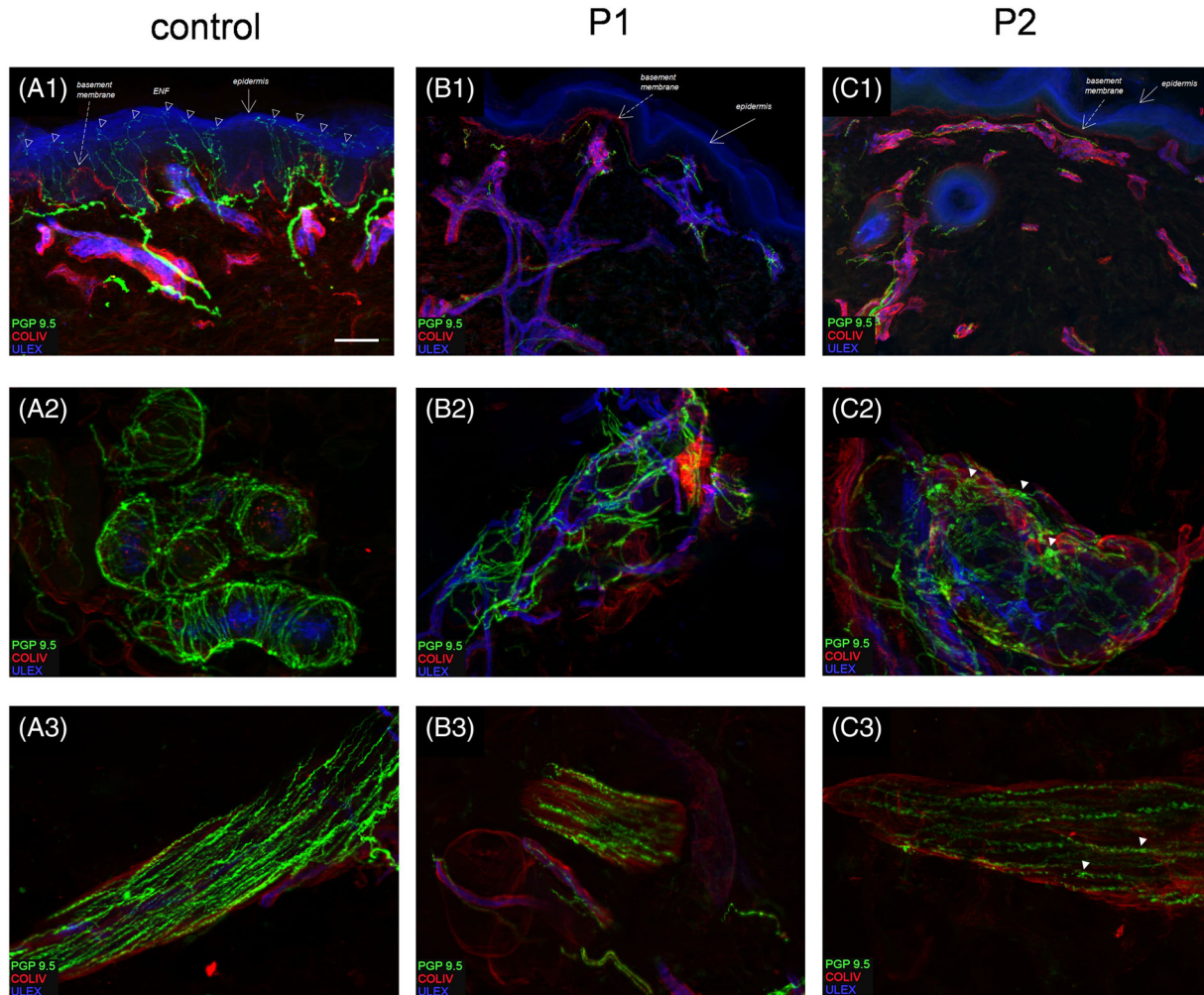


FIGURE 3 Study of skin innervation. (A–C) Digital confocal images from a distal site showing epidermal and dermal innervation in a young healthy control (A) and in the patients carrying p.S331 variants in the *SPTLC1* gene (B, C). (A1–C1) Epidermal nerve fibres (ENF - empty arrowheads in A1) are completely absent in patients' skin (B1, C1) compared with the control (A1). A severe reduction of nerves around sweat glands (B2, C2) and along *erector pili* muscles (B3, C3) is also evident in patients compared with the healthy subject (A2, A3). The image series 1 at lower magnification (10 \times) show the extent of epidermis and dermis denervation in both patients compared with the control; the image series 2 and 3 show at higher magnification (20 \times) the morphological abnormalities of sudomotor and pilomotor nerves in terms of cotton-like aspect, more evident in patient two (full arrowhead in C2 and C3) compared with the control (A2, A3). In green: nerves marked with the pan-neuronal protein gene product 9.5 (PGP9.5) antibody. In red: basement membrane and blood vessels marked with Collagen IV (Col IV) antibody. In blue: endothelia and epidermis marked with *ULEX europaeus*. Bar A1–C1 = 100 μ m, A2–C2, A3–C3 = 50 μ m

derived fibroblasts. We used 3,3-D₂ L-serine and D₄ L-alanine to assess de novo rates of SLs and 1-deoxySLs synthesis in p.S331 variant fibroblasts, respectively. This experiment showed elevated levels of D₂ containing SLs in p.S331 cells compared with controls, suggestive of increased activity of p.S331-containing SPT (Figure 6A).

Consistent with the serum data, p.S331 fibroblasts also synthesised elevated levels of 1-deoxy and 1-deoxymethyl SLs, suggestive of increased alanine usage by the p.S331 mutant SPT (Figure 6B). Given the known clinical benefit from serine supplementation in typical HSAN patients, we tested the effects of serine supplementation on SL synthesis. Addition of L-serine reduced the levels of 1-deoxySA and 1-deoxyCer in p.S331Y fibroblasts but did not affect

these levels in p.S331F fibroblasts. In contrast, L-serine addition increased the levels of SA and total ceramide in p.S331F cells without dramatically affecting their levels in p.S331Y cells or control cells (Figure 6C).

DISCUSSION

Inherited peripheral neuropathies are divided into three main subclasses based on the predominant involvement of motor or sensory and autonomic neurons: hereditary motor and sensory neuropathies (HMSN), hereditary motor neuropathies (HMN) and hereditary sensory and autonomic neuropathies (HSAN).¹⁹

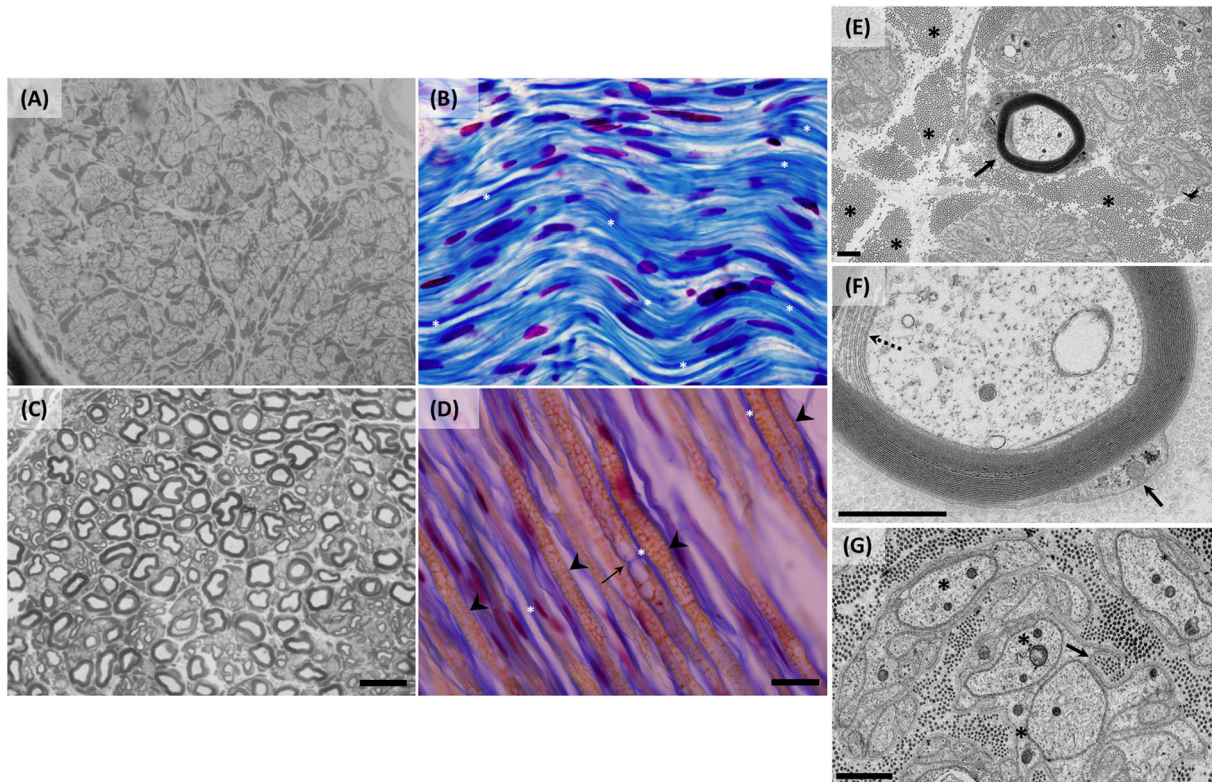


FIGURE 4 Neuropathological study of patient one's sural nerve biopsy. (A, C) Semithin sections of sural nerve biopsy (Toluidine blue; scale bars = 20 μm) from Patient 1 (A) display a complete loss of myelinated fibres compared with control subject (C). (B, D) Paraffin-embedded longitudinal sections of sural nerve biopsy from Patient 1 (B) and a control subject (D) were stained with Mallory trichrome to show myelinated fibres (gold yellow), collagen fibrils (deep blue) and nuclei (red). Patient 1 displays a complete loss of myelinated fibres that are clearly identifiable in the control (D, black arrowheads) as well as nodes of Ranvier (D, black arrow). Instead, a massive deposition of collagen is present in Patient 1 compared with the control subject (B, white asterisks). Bar in B, D = 20 μm . (E–G) TEM on sural nerve biopsy of Patient 1 shows a remarkable increase of collagen fibrils (E, black asterisks); strikingly, we found only one myelinated fibre in all the nerve fascicles (E, black arrow). At higher magnification (F), this myelinated fibre displays clear signs of degeneration both in the Schwann cell cytoplasm (F, black arrow) and at axon level with detachment from the myelin membrane (F, black dotted arrow). (G) Unmyelinated fibres did not show signs of suffering. Occasionally, we detected collagen pockets (G, black arrow). An increased number of mitochondria was also found (G, black asterisks). Bar in E–G = 1 μm

Patients with HSAN typically manifest with loss of sensation and autonomic dysfunction and no or mild motor involvement. The most common form of this category is HSAN1 secondary to pathogenic variants in *SPTLC1*.

Distinct variants in *SPTLC1* have been recently associated with juvenile ALS, presenting with childhood-onset motor neuron disease without clinical, electrophysiological or pathological evidence of sensory neuropathy. Notably, all of these recently identified ALS-associated *SPTLC1* variants cluster in exon two of *SPTLC1* and have a different effect on SPT enzyme activity when compared with HSAN1 variants in the same gene: while HSAN1 variants alter the substrate preference of SPT from L-serine to L-alanine and glycine, ALS associated variants result in an overactive SPT and overproduction of SLs.¹⁰

The amino acid serine at position 331 in exon 11 is emerging as a unique hotspot for *SPTLC1*, with a distinct phenotype, namely, 'S331 syndrome' manifesting with early onset motor phenotype, growth retardation and sensory-autonomic impairment. A detailed

histopathological analysis in nerve and skin samples has not yet been described in such patients.

The p.S331Y variant was first described in a 14-year-old girl with a progressive muscle weakness and wasting leading to severe scoliosis, respiratory insufficiency and loss of ambulation.¹ A second patient was also reported, sharing most of the p.S331 core clinical characteristics, including early onset of diffuse muscle weakness, atrophy and cataracts¹¹ (Table 1).

Our patient with p.S331Y variant (Patient 1) initially manifested with mild sensory impairment displaying pain and discomfort to touch at age 4 years. She subsequently developed progressive weakness with brisk reflexes and tongue fasciculation, analogous to the two others reported patients with p.S331Y mutation, suggestive of a concomitant motor neuropathy. She showed neither sign of autonomic involvement nor cataracts.

The p.S331F variant was first reported in a patient with congenital phenotype of severe growth retardation, global amyotrophy, cataracts, microcephaly and respiratory involvement.¹² Two additional

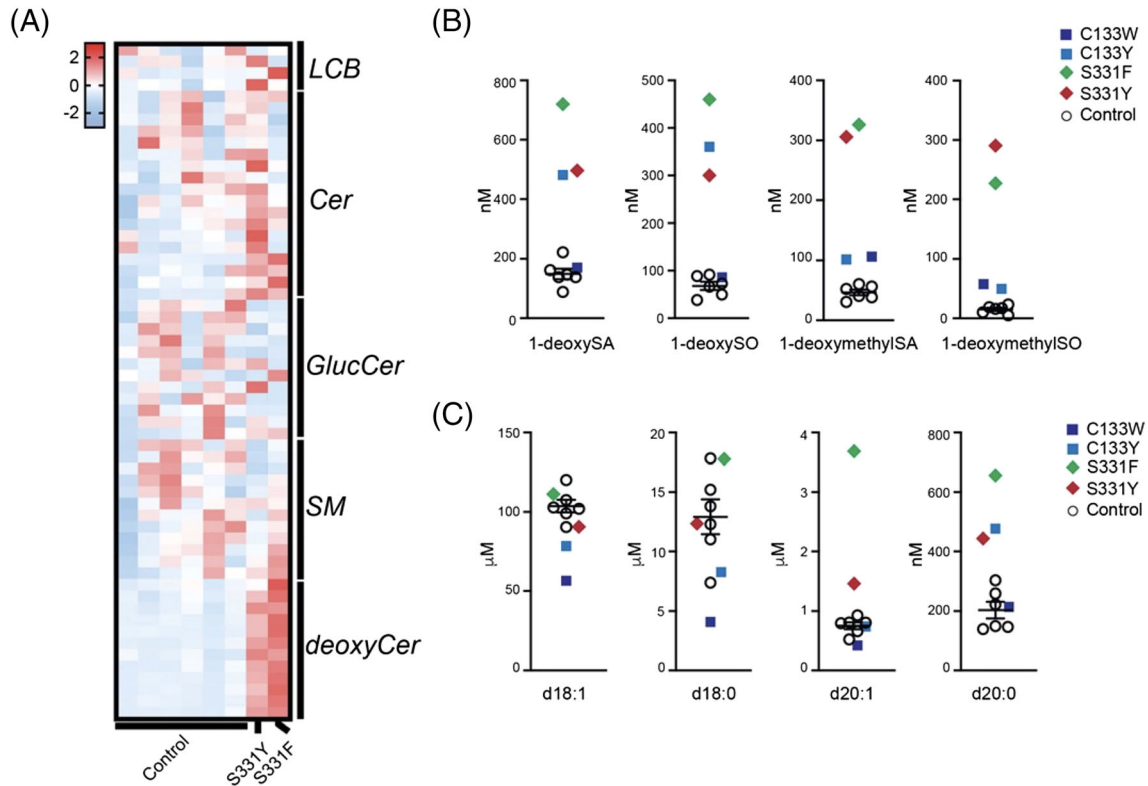


FIGURE 5 Sphingolipidomic analysis of serum samples of patients with SPTLC1 p.S331 variants. (A) HPLC-MS analysis of serum samples with each row representing a different sphingolipid species. Row Z-scores were generated and depicted in a heatmap form. LCB, long chain base; Cer, ceramides; GlucCer, glucosylceramides; SM, sphingomyelins; deoxyCer, 1-deoxyCeramides. (B) Serum levels of 1-deoxy and 1-deoxymethyl long chain bases after acid hydrolysis in control, classic HSAN1 (SPTLC1 p.C133Y/W) and SPTLC1 p.S331 samples. SA, sphinganine; SO, sphingosine. (C) Serum levels of C-18 (d18:1 and d18:0) and C-20 (d20:1 and d20:0) long chain bases after acid hydrolysis in control, classic HSAN1 (SPTLC1 p.C133Y/W) and SPTLC1 p.S331 samples

patients have been described: a French boy with severe growth and cognitive involvement and vocal cord paralysis, and a patient of German origin with insensitivity to pain, anhidrosis and progressive motor impairment.^{20,21}

Very recently, the p.S331F variant has been reported in a single patient with 'juvenile ALS plus syndrome'.²² In particular, the authors described not only upper and lower motor neuron signs but also autonomic and sensory disturbances such as hyperhidrosis, insensitivity to pain, and foot ulceration.²²

Our patient with p.S331F variant (Patient 2) presented with an infantile onset of global clumsiness and signs of autonomic dysfunction characterised by altered gastrointestinal motility, hypohidrosis and keratoconjunctivitis sicca with corneal ulcers.

Although she was still able to walk independently, diffuse hypotonia, foot deformity, muscle biopsy and MRI findings were indicative of motor system involvement.

Sensory impairment, albeit not manifesting symptomatically, was evident on nerve conduction studies and from the neuropathological findings on skin biopsy. Our skin innervation study from both patients showed a complete lack of epidermal nerve fibres. We also report a complete lack of myelinated fibres and a severe involvement of autonomic nerve fibres worst in the younger patient with the

p.S331F mutation in line with the more severe autonomic dysfunction.

Histopathological characterisation of SPTLC1-related HSAN1 is available only from patients harbouring the common p.C133W variant.²³ These studies display similar neuropathological abnormalities with very few myelinated fibres, a relative greater preservation of unmyelinated axons, and extremely rare signs of regeneration. In contrast, a SPTLC1-related ALS patient was reported to have a normal sural nerve.¹⁰ Our neuropathological study of patient with p.S331Y mutation at both light and electron microscopy highlighted a severe phenotype with a complete loss of myelinated fibres (in line with the skin findings) and increased amount of collagen fibrils inside the endoneurium. The picture is similar to classic HSAN1 although myelinated fibres seem to be more severely affected in our patient with just a single spared myelinated fibre. Conversely, unmyelinated fibres were preserved. This aspect is in apparent contrast with the complete lack of somatic unmyelinated fibres and the severe involvement of autonomic nerve fibres in skin samples. However, it is possible that during development the unmyelinated fibres do not properly reach their target or that their distal endings degenerated early due to the toxic effect of SLs.

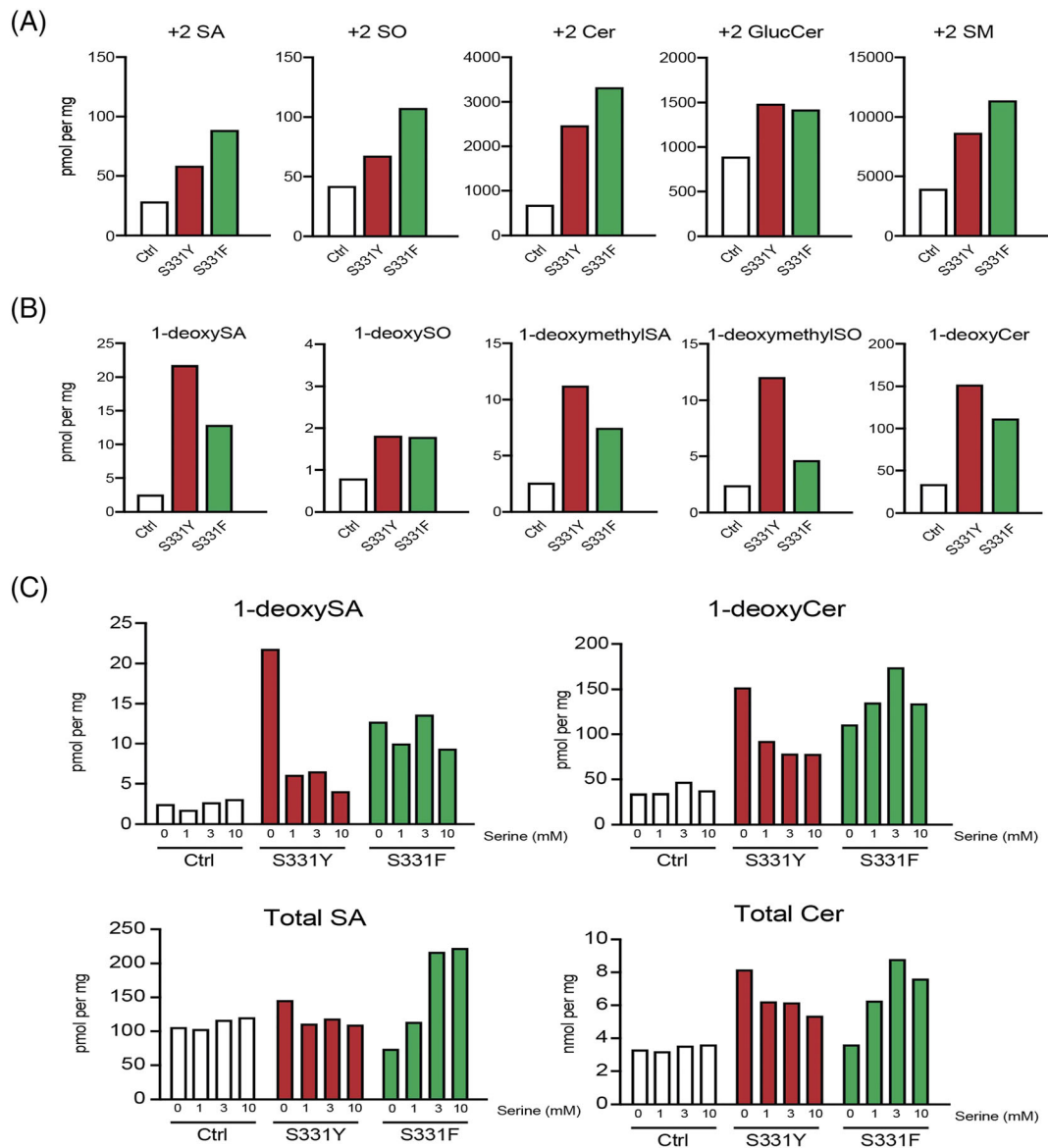


FIGURE 6 Spingolipidomic analysis of patient derived fibroblasts with SPTLC1 p.S331 variants. (A) HPLC-MS lipidomic analysis of fibroblasts harvested after 3,3-D2 L-serine treatment (3mM). Only the D2-containing (+2) species were quantified to reflect the de novo rate of synthesis for each species. SA, sphinganine; SO, sphingosine; Cer, ceramide; GlucCer, glucosylceramides; SM, sphingomyelin. (B) HPLC-MS lipidomic analysis of fibroblasts harvested after D4-alanine (3 mM) supplementation. Only the D3-containing (+3) deoxysphingolipid species were quantified to reflect the de novo rate of synthesis for each species. DHC, dihydroceramide. (C) The effect of increasing L-serine supplementation on deoxy sphingolipids, total sphinganine and total ceramide levels in S331 fibroblasts. The height of columns represents the average of two technical replicates.

Overall, detailed clinical and neuropathological phenotyping of our patients suggest that p.S331 *SPTLC1* variants may represent a continuum in the *SPTLC1*-associated spectrum manifesting with a severe and early onset mixed sensory and motor phenotype, including clinical and pathological features of both HSAN1 and ALS (Figure 7 and Table 2).

From a biochemical perspective, different *SPTLC1* variants exert different effects on the SPT enzyme.^{10,14} Typical HSAN1 pathogenic variants cause a shift from the use of canonical substrate serine to the use of non-canonical alanine and glycine, forming two atypical

sphingoid bases: 1-deoxy-sphinganine (1-deoxySA) and 1-deoxymethyl-sphinganine (1-deoxymethylSA).⁸ Elevated 1-deoxySL levels in plasma and lymphoblasts of typical HSAN1 patients thus represent a biochemical hallmark of HSAN1 and a candidate biomarker for this disease.²⁴ Similar to classic patients affected by HSAN1, toxic 1-deoxySLs are also increased in the serum of patients with p.S331 mutations, indicating an analogous pathogenic mechanism. Indeed, both our patients displayed increased level of 1-deoxy and 1-deoxymethylSLs in the serum and elevated rates of de novo 1-deoxySLs synthesis without any differences between p.S331Y and

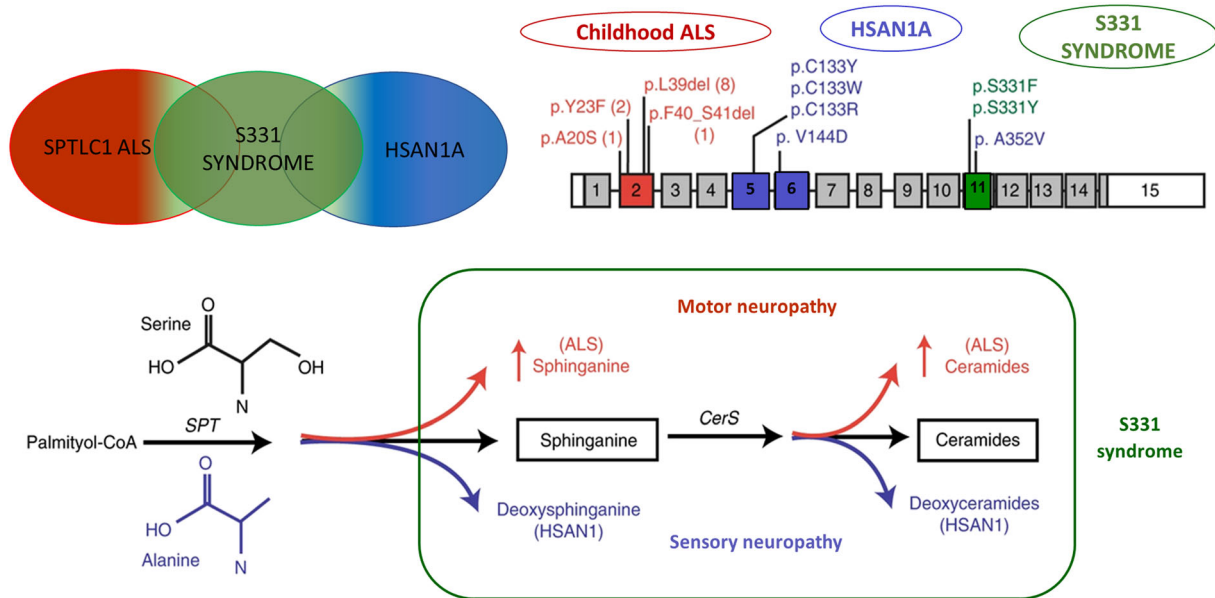


FIGURE 7 Genotype–phenotype correlation in SPTLC1 related disorders. S331 SPTLC1 phenotype shares HSAN and ALS features with clinical, electrophysiology, neuropathology and biochemical overlap, confirming SPTLC1 related disorders spectrum range from sensory autonomic neuropathy to pure motor neuron disease depending on site and effect of the different gene mutations.

TABLE 2 Comparison of the genetic, clinical, histopathological and biochemical features among the different SPTLC1 related disorders

	Typical HSAN1A	Ser331 SPTLC1	SPTLC1-ALS
SPTLC1 mutation site	Exon 5 and 6	Exon 11	Exon 2
Age at onset	Juvenile/Adult onset	Early childhood/Infantile	Childhood
Sensory-autonomic neuropathy	Yes	Yes	No
Diffuse muscular atrophy	No	Yes	Yes
Progressive motor neuropathy	No	Yes	Yes
Nerve conduction study	Mixed axonal and demyelinating sensory-motor length dependent neuropathy	Severe demyelinating UL and LL Absent sensory responses LL	Normal nerve conduction
Muscle biopsy	NA	Predominance of type 1 fibres. Denervation	Type grouping and denervation
Sural nerve biopsy	Marked wasting of myelinated fibres, unmyelinated fibres were present	Complete depletion of myelinated fibres and a remarkable hypertrophy of connective tissue with collagen-pocket structure	No abnormalities in myelinated or unmyelinated sensory nerve fibres
Skin biopsy	Reduced cutaneous innervation in a length-dependent pattern	Complete loss of epidermal nerve fibres and reduced autonomic innervation	Not performed
Serum sphingolipids chances and SPT activity	Increased deoxySL levels	Increased 1-deoxySL levels, increased SPT activity and canonical SPT products	Normal deoxySL levels; increased SPT activity and canonical SPT products
Response to L-serine supplementation	Biochemical improvement with significant reduction of 1-deoxySL levels and an increase in epidermal innervation	Different effect on S331Y and S331F patients' fibroblast. Biochemical improvement in S331Y with reduction of 1-deoxySL and sphingolipid levels. Biochemical worsening with no effect in S331F	Biochemical worsening with increase of the already elevated sphingolipid levels

p.S331F variants. This biochemical finding will likely account for sensory and autonomic deficit symptoms identified in our patients, similar to classic HSAN1.

Increased activity of SPT has recently been associated with ALS and motor neuropathy without sensory nerve involvement,¹⁰ leading us to speculate that the motor phenotype noted in patients with p.S331 variants (and absent in patients with classic HSAN1) may be due to the secondary effect of these variants on SPT activity and increased SLs synthesis. The pathogenic effect of p.S331 mutations on SPT activity has been previously investigated in vitro with conflicting results.^{14,21} Using a transient overexpression model, Rotthier demonstrated a reduced SPT activity in p.S331 transfected cells.²¹ However, when comparing the enzymatic properties using a uniform isotope labelling approach in transfected HEK293 cells, p.S331F and p.S331Y SPT mutants were associated with increased canonical activity including increase of both C18- and C20-sphingoid base synthesis.¹⁴ We also identified an increased level of C20-sphingoid bases in the patient serum samples and increased rates of de novo synthesis of canonical SPT products in patient-derived cells without the limitations of transient transfection and overexpression of prior studies.^{14,21}

Taken together these considerations support the hypothesis that the distinct *SPTLC1* associated phenotypes are caused by the different biochemical consequences of SPT variants. In particular, the increase of toxic 1-deoxySLs may account for the sensory-autonomic neuropathy, while SPT over-activity and perhaps C20-sphingoid base synthesis could affect the motor neurons leading to the motor phenotype in our patients. We do not yet understand why motor and sensory neurons show selective vulnerability to distinct biochemical changes in SL synthesis and homeostasis. Further work is needed to clarify the pathomechanism of p.S331 variants on SPT regulation including how the change of this specific amino acid leads to the substrate shift and the apparent lack of inhibition.

Understanding the exact consequences of the *SPTLC1* variants, including p.S331, on SL synthesis is fundamental also for pursuing therapeutic intervention such as serine supplementation. Indeed, early intervention may prohibit further deterioration due to toxic SL accumulation, and this is particularly relevant for these early onset cases which are typically associated with rapid progression. For this purpose, we tested the effect of L-serine supplementation on toxic SLs in patient fibroblasts. Production of 1-deoxySO and 1-deoxySA was reduced only in the cells of patient with p.S331Y mutation and otherwise remained unchanged. In contrast, addition of L-serine increased the rate of canonical SL synthesis in p.S331F cells. Since increased SPT activity and overproduction of canonical SLs are thought to be responsible for the motor component of the disease, serine supplementation may worsen the motor neuron disease and thus should be avoided in these patients.

CONCLUSION

We have presented detailed clinical and biochemical data, combined with sural nerve and cutaneous pathology to further characterise

patients with the *SPTLC1* p.S331 mutations. The biochemical analysis in our patients harbouring the p.S331 variants showed mixed findings of both an elevation of 1-deoxySLs as in HSAN1, and increased levels of canonical SPT products as in ALS patients.

From these results, we suggest that the p.S331 variants bridge a clinical overlap of classic HSAN1 and the recently reported childhood-onset ALS. We have also demonstrated that L-serine supplementation in fibroblasts of patients with p.S331 mutations results in increase of canonical SL synthesis and thus may worsen the motor phenotype.

ACKNOWLEDGEMENTS

We acknowledge the following: Care4NeuroRare (CP 20/2018) from FRRB to FT; French Muscular Dystrophy Association grant 22431 to CF and SB; and Italian Ministry of Health Ricerca corrente 2018-2021 to LN.

CONFLICT OF INTEREST

Nothing to report.

ETHICS STATEMENT

Written informed consent for the above-mentioned research studies and for image use were obtained from patients' parents according to WMA Helsinki Declaration 2013. The study has been approved by local research ethic committee.

AUTHOR CONTRIBUTIONS

CF: conception and design of the study, acquisition and analysis of data, drafting of the manuscript. GC: conception and design of the study, acquisition and analysis of data, drafting of the manuscript. AG: acquisition and analysis of genetic data, drafting of the manuscript. IM: acquisition and analysis of clinical data, drafting of the manuscript. PM: conception and design of the study, acquisition and analysis of data, drafting of the manuscript. MC: acquisition and analysis of neurophysiological data. CC: acquisition and analysis of neurophysiological data. SM: acquisition and analysis of neuropathy scales. CP: acquisition and analysis of clinical data. MP: acquisition and analysis of clinical data. NB: acquisition and analysis of clinical data and skin biopsy. SS: acquisition and analysis of muscle biopsy data. MT: acquisition and analysis of genetic data. SB: acquisition and analysis of muscle biopsy data. DD: acquisition and analysis of nerve biopsy electron microscopy data. SM: acquisition and analysis of genetic data. ST: acquisition and analysis of clinical and skin biopsy data, drafting the manuscript. VP: acquisition and analysis of clinical data. EB: acquisition and analysis of genetic data. VS: conception and design of the study, drafting the manuscript. SD: drafting the manuscript. KG: acquisition and analysis of biochemical data. SDG: acquisition and analysis of biochemical data. TMD: acquisition and analysis of biochemical data, drafting the manuscript. CGB: conception and design of the study, drafting the manuscript. FT: acquisition and analysis of genetic data, drafting the manuscript. AS: acquisition and analysis of neuropathology data, drafting the manuscript. PM: acquisition and analysis of genetic data, drafting the manuscript. LN: conception and design of the study, acquisition and analysis of neuropathology data, drafting

the manuscript. MN: conception and design of the study, acquisition and analysis of skin biopsy data, drafting the manuscript.

PEER REVIEW

The peer review history for this article is available at <https://publons.com/publon/10.1111/nan.12842>.

DATA AVAILABILITY STATEMENT

The data supporting the findings of this study are available from the corresponding author upon request.

ORCID

Chiara Fiorillo  <https://orcid.org/0000-0001-9027-343X>

Lucilla Nobbio  <https://orcid.org/0000-0003-2150-3953>

REFERENCES

- Hanada K. Serine palmitoyltransferase, a key enzyme of sphingolipid metabolism. *Biochim Biophys Acta*. 2003;1632(1-3):16-30. doi:10.1016/s1388-1981(03)00059-3
- Hojjati MR, Li Z, Jiang XC. Serine palmitoyl-CoA transferase (SPT) deficiency and sphingolipid levels in mice. *Biochim Biophys Acta*. 2005;1737(1):44-51. doi:10.1016/j.bbalip.2005.08.006
- Visigalli D, Capodivento G, Basit A, et al. Exploiting sphingo- and glycerophospholipid impairment to select effective drugs and biomarkers for CMT1A. *Front Neurol*. 2020;11:903. Published 2020 Aug 25. doi:10.3389/fneur.2020.00903
- Auer-Grumbach M, Bode H, Pieber TR, et al. Mutations at Ser331 in the HSN type I gene SPTLC1 are associated with a distinct syndromic phenotype. *Eur J Med Genet*. 2013;56(5):266-269. doi:10.1016/j.ejmg.2013.02.002
- Fridman V, Oaklander AL, David WS, et al. Natural history and biomarkers in hereditary sensory neuropathy type 1. *Muscle Nerve*. 2015;51(4):489-495. doi:10.1002/mus.24336
- McC Campbell A, Truong D, Broom DC, et al. Mutant SPTLC1 dominantly inhibits serine palmitoyltransferase activity in vivo and confers an age-dependent neuropathy. *Hum Mol Genet*. 2005;14(22):3507-3521. doi:10.1093/hmg/ddi380
- Gable K, Gupta SD, Han G, Niranjanakumari S, Harmon JM, Dunn TM. A disease-causing mutation in the active site of serine palmitoyltransferase causes catalytic promiscuity. *J Biol Chem*. 2010;285(30):22846-22852. doi:10.1074/jbc.M110.122259
- Penno A, Reilly MM, Houlden H, et al. Hereditary sensory neuropathy type 1 is caused by the accumulation of two neurotoxic sphingolipids. *J Biol Chem*. 2010;285(15):11178-11187. doi:10.1074/jbc.M109.092973
- Fridman V, Suriyanarayanan S, Novak P, et al. Randomized trial of l-serine in patients with hereditary sensory and autonomic neuropathy type 1. *Neurology*. 2019;92(4):e359-e370. doi:10.1212/WNL.0000000000006811
- Mohassel P, Donkervoort S, Lone MA, et al. Childhood amyotrophic lateral sclerosis caused by excess sphingolipid synthesis. *Nat Med*. 2021;27(7):1197-1204. doi:10.1038/s41591-021-01346-1
- Rossi F, Bruno G, Fratta M, et al. Expanding the spectrum of SPTLC1-related disorders beyond hereditary sensory and autonomic neuropathies: a novel case of the distinct "S331 syndrome". *J Peripher Nerv Syst*. 2020;25(3):308-311. doi:10.1111/jns.12394
- Rotthier A, Baets J, De Vriendt E, et al. Genes for hereditary sensory and autonomic neuropathies: a genotype-phenotype correlation. *Brain*. 2009;132(Pt 10):2699-2711. doi:10.1093/brain/awp198
- Suh BC, Hong YB, Nakhro K, Nam SH, Chung KW, Choi BO. Early-onset severe hereditary sensory and autonomic neuropathy type 1 with S331F SPTLC1 mutation. *Mol Med Rep*. 2014;9(2):481-486. doi:10.3892/mmr.2013.1808
- Bode H, Bourquin F, Suriyanarayanan S, et al. HSN1 mutations in serine palmitoyltransferase reveal a close structure-function-phenotype relationship. *Hum Mol Genet*. 2016;25(5):853-865. doi:10.1093/hmg/ddv611
- Yang H, Wang K. Genomic variant annotation and prioritization with ANNOVAR and wANNOVAR. *Nat Protoc*. 2015;10(10):1556-1566. doi:10.1038/nprot.2015.105
- Nolano M, Tozza S, Caporaso G, Provitera V. Contribution of Skin Biopsy in Peripheral Neuropathies. *Brain Sci*. 2020;10(12):989. doi:10.3390/brainsci10120989
- Sommer CL, Brandner S, Dyck PJ, et al. Peripheral nerve society guideline on processing and evaluation of nerve biopsies. *J Peripher Nerv Syst*. 2010;15(3):164-175. doi:10.1111/j.1529-8027.2010.00276.x
- Merrill AH Jr, Sullards MC, Allegood JC, Kelly S, Wang E. Sphingolipidomics: high-throughput, structure-specific, and quantitative analysis of sphingolipids by liquid chromatography tandem mass spectrometry. *Methods*. 2005;36(2):207-224. doi:10.1016/j.ymeth.2005.01.009
- Reilly MM. Sorting out the inherited neuropathies. *Pract Neurol*. 2007;7(2):93-105.
- Rotthier A, Auer-Grumbach M, Janssens K, et al. Mutations in the SPTLC2 subunit of serine palmitoyltransferase cause hereditary sensory and autonomic neuropathy type I. *Am J Hum Genet*. 2010;87(4):513-522. doi:10.1016/j.ajhg.2010.09.010
- Rotthier A, Penno A, Rautenstrauss B, et al. Characterization of two mutations in the SPTLC1 subunit of serine palmitoyltransferase associated with hereditary sensory and autonomic neuropathy type I. *Hum Mutat*. 2011;32(6):E2211-E2225. doi:10.1002/humu.21481
- Johnson JO, Chia R, Miller DE, et al. Association of variants in the SPTLC1 gene with juvenile amyotrophic lateral sclerosis. *JAMA Neurol*. 2021;78(10):1236-1248. doi:10.1001/jamaneurol.2021.2598
- Houlden H, King R, Blake J, et al. Clinical, pathological and genetic characterization of hereditary sensory and autonomic neuropathy type 1 (HSAN I). *Brain*. 2006;129(Pt 2):411-425. doi:10.1093/brain/awh712
- Boso F, Armirotti A, Taioli F, et al. Deoxysphingolipids as candidate biomarkers for a novel SPTLC1 mutation associated with HSN-I. *Neurol Genet*. 2019;5(6):e365. doi:10.1212/NXG.0000000000000365

How to cite this article: Fiorillo C, Capodivento G, Geroldi A, et al. The SPTLC1 p.S331 mutation bridges sensory neuropathy and motor neuron disease and has implications for treatment. *Neuropathol Appl Neurobiol*. 2022;e12842. doi:10.1111/nan.12842